

Proxitaxis: an adaptive search strategy based on proximity and stochastic resetting

Giuseppe Del Vecchio Del Vecchio,^{1,*} Manas Kulkarni,^{2,†} Satya N. Majumdar,^{1,‡} and Sanjib Sabhapandit^{3,§}

¹*LPTMS, CNRS, Université Paris-Sud, Université Paris-Saclay, 91405 Orsay, France*

²*International Centre for Theoretical Sciences, Tata Institute of Fundamental Research, Bangalore 560089, India*

³*Raman Research Institute, Bangalore 560080, India*

(Dated: July 9, 2025)

We introduce *proxitaxis*, a simple search strategy where the searcher has only information about the distance from the target but not the direction. The strategy consists of three crucial components: (i) local adaptive moves with distance-dependent hopping rate, (ii) intermittent long range returns via stochastic resetting to a certain location \vec{R}_0 , and (iii) an inspection move where the searcher dynamically updates the resetting position \vec{R}_0 . We compute analytically the capture probability of the target within this strategy and show that it can be maximized by an optimal choice of the control parameters of this strategy. Moreover, the optimal strategy undergoes multiple phase transitions as a function of the control parameters. These phase transitions are generic and occur in all dimensions.

Search problems are ubiquitous in nature [1–6]. There are several examples where the searcher may have only partial information about the target. For instance, from some locally available cues, the searcher might be able to infer its distance from the target (mobile or immobile), but not the direction in which the target is located. A classic example of such search processes with incomplete information is the so-called ‘infotaxis’ [7–10], where unlike chemotaxis [11–14], there is no strong concentration gradient to guide the searcher towards the target. This could be due to the existence of winds or turbulence that leads to sporadic or intermittent arrival of signals. Examples of such search processes with only partial information can be found in many contexts [15–19]. These include the search of a shipwreck deep inside the ocean using acoustic sensors, detection of a source of radioactivity or a gas leak, seismic exploration, and olfactory searches by animals. In all these examples, the local sensor can give an estimate of its distance from the source, but not the direction in which the source is located. Thus, it is important and of practical relevance to engineer a search protocol where the searcher only has instantaneous information about the distance to the target.

In this Letter, we propose a new search strategy that works efficiently with this limited information *only* about distance from the source. We call this ‘proxitaxis’ (inspired by the terminologies like chemotaxis and infotaxis), where ‘proxi’ refers to proximity to the target and ‘taxis’ to the movement of the searcher in response to stimuli.

One crucial ingredient of our *proxitaxis* strategy is drawn from the so-called intermittent search protocol [20–23], where the searcher employs two types of moves intermittently: (a) local short-ranged stochastic jumps typically modeled by diffusion where the searcher

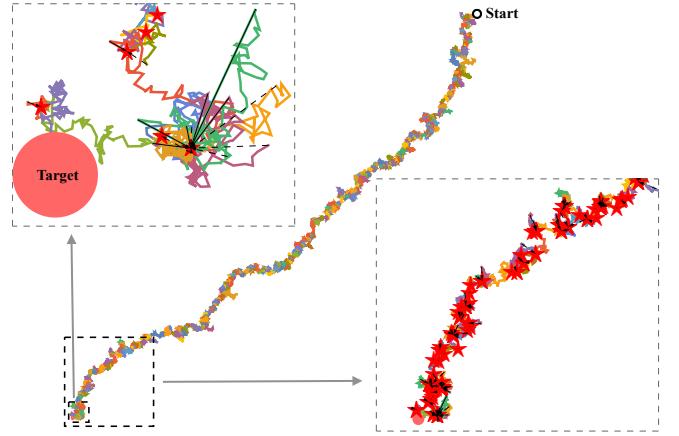


Figure 1. A typical trajectory generated by the *proxitaxis* search strategy in two dimensions. The single target is shown by the red disk and the searcher’s initial location is indicated by the black circle. The central figure shows the trajectory over a large length and time scale, illustrating that the strategy guides the searcher almost deterministically towards the target. However, on smaller scales, one sees fluctuations. For example, the top box zooms the trajectory close to the target, where the searcher becomes more active. In contrast, the right box zooms the trajectory at some intermediate scales where it is less active, i.e., more sluggish. See the main text for the details of the strategy.

tries to locate the target and (b) long-range moves during which it does not search but relocates to a different region of space. One popular model that incorporates these two intermittent moves, and yet analytically tractable, is *diffusion with stochastic resetting* [24–31] that attracted much attention in recent times. In this model, the searcher performs Brownian diffusion (local moves) and with a constant rate resets instantaneously to its initial position (long-range moves) and restarts the search. The rationale is that when one restarts the search process, one may find a better pathway that leads to the target in a shorter time. In many model systems, it has been established that the stochastic resetting typically

* giuseppe.del-vecchio-del-vecchio@universite-paris-saclay.fr

† manas.kulkarni@icts.res.in

‡ satya.majumdar@universite-paris-saclay.fr

§ sanjib@rri.res.in

expedites the search of a target [24–30, 32], see however [33–35] for the conditions on the existence of a nonzero optimal resetting rate. Some of the analytical predictions have also been verified recently in experiments using colloidal particles in optical traps [36–38].

In the standard model of diffusion with stochastic resetting [24, 25], the diffusion constant associated with the local hopping is assumed to be space-independent. However, in many situations, the searcher may want to use an adaptive strategy whereby its rate of local activity increases as it approaches the target. For example, during the foraging period, animals are known to modify their movements when they get closer to their targets [39, 40]. Far from the target, the movement is typically slow or sluggish with a lower hopping rate allowing a broader local exploration. However, when the animal gets closer to the target, it can detect cues such as smell or sound, which may trigger faster and more active movements with larger hopping rates, allowing them to scan for the target more intensively. This increase in the hopping rate or higher activity/motility closer to the target is an example of a dynamic adjustment in the exploration process, a common phenomenon in various biological, cognitive, ecological and even financial contexts [41–44]. In principle, the searcher can choose different strategies of local movements depending on its distance from the target. For example, it can change its behavior from diffusive to ballistic when it nears the target [19]. However, this alone is not enough. If it moves ballistically, without knowing the direction but only the distance from the source, it will surely miss the target. Hence, besides incorporating distance-dependent local moves, the searcher needs an additional strategic move that does not require the knowledge of the direction. Such a move is indeed provided by stochastic resetting to the initial position, which only requires, in addition to the initial position of the searcher, the distance from the target but not the direction in which it is located.

These two components, namely the distance-dependent local exploration and stochastic resetting to the initial location \vec{R}_0 , are, however, not enough to ensure an efficient search since the walker has at its disposal the information about its instantaneous distance from the target. It makes no sense to reset to \vec{R}_0 if its current distance $R(t) < R_0 = \|\vec{R}_0\|$. Therefore, the searcher should ideally compare its current distance $R(t)$ to R_0 and should reset to \vec{R}_0 only if $R(t) > R_0$. Moreover, to make the search more efficient, the walker should also dynamically update its resetting position from \vec{R}_0 to $\vec{R}(t)$ if $R(t) < R_0$. It is, however, highly costly and hence inefficient to do this comparison at every step. It is natural to assume that there is a typical time scale associated with this inspection process, which depends on the animal’s processing ability. Here we simply assume that this inspection happens intermittently at Poisson distributed times with a rate b .

In this Letter, we propose *proxitaxis* as a possible new search strategy based on these three aspects of a realistic

search with only information about the distance from the target. The *proxitaxis* protocol is essentially a recursive search strategy with memory. One starts with a sequence of time intervals $\{\tau_1, \tau_2, \dots\}$, each drawn independently from a common distribution $p(\tau) = b e^{-b\tau}$. Let $\vec{R}_0^{(i)}$ denote the position of the walker at the beginning of an interval τ_i . Within each interval τ_i , the strategy consists of two moves: (1) local diffusion with a hopping rates $D_i(R)$ that increases as the instantaneous distance R from the target decreases and (2) long range stochastic resetting with a constant rate r_i to the position $\vec{R}_0^{(i)}$ at the beginning of the time interval τ_i (indicated by the black arrows in Fig. 1). If the searcher finds the target within time τ_i the process ends. Otherwise, the strategy repeats for the next interval τ_{i+1} with a new initial and resetting position $\vec{R}_0^{(i+1)}$ chosen as follows: $\vec{R}_0^{(i+1)} = \vec{R}(t_i)$ if $R(t_i) < R_0$ else $\vec{R}_0^{(i+1)} = \vec{R}_0^{(i)}$ (indicated by the dashed arrows in Fig. 1), where $t_i = \tau_1 + \tau_2 + \dots + \tau_i$ is the actual time at the end of the i -th interval. This inspection move is indeed the third important component of the *proxitaxis* strategy. Thus, in this strategy, the resetting location is dynamically updated via the inspection move, thereby creating an overall drift towards the target, making the strategy highly effective [see Fig. 1, where the sequence of $R_0^{(i)}$ ’s are marked by the red stars]. Within each random interval τ_i , an efficient searcher should choose the control parameters $\{D_i(R), r_i\}$ to maximize its chance of capturing the target. Solving analytically a simple d -dimensional model, we show that the capture probability within each interval τ_i can indeed be optimized by a suitable choice of the control parameters $\{D_i(R), r_i\}$ in any dimension. With this choice of the optimal control parameters, the *proxitaxis* search strategy can then be made efficient in all dimensions.

Since we optimize the parameters $\{D_i(R), r_i\}$ independently within each time interval τ_i , to find the optimal parameters one can just focus on a single interval. Therefore, we will drop the index i labeling the intervals in what follows. We consider a searcher in d -dimensions in the presence of a spherical target of radius $\epsilon > 0$. Since only the relative position between the searcher and the target matters, without loss of generality, we place the target at the origin. Let \vec{R}_0 be the position of the searcher at the beginning of the interval. The position $\vec{R}(t)$ of the searcher evolves via the following dynamics. In a small time interval $[t, t + \Delta t]$ it resets to \vec{R}_0 with probability $r\Delta t$ and with the complementary probability $1 - r\Delta t$ it diffuses with diffusion coefficient $D(R(t))$ that depends only on the distance $R(t) = \|\vec{R}(t)\|$ of the instantaneous position of the searcher from the target. The search process terminates when the searcher hits the boundary of the target, i.e., when $R(t) = \epsilon$. However, within the interval τ , the searcher may or may not find the target. In order to characterize the efficiency of the strategy, we maximize the capture probability $C(\vec{R}_0)$ defined as the probability that the target is captured within the life-

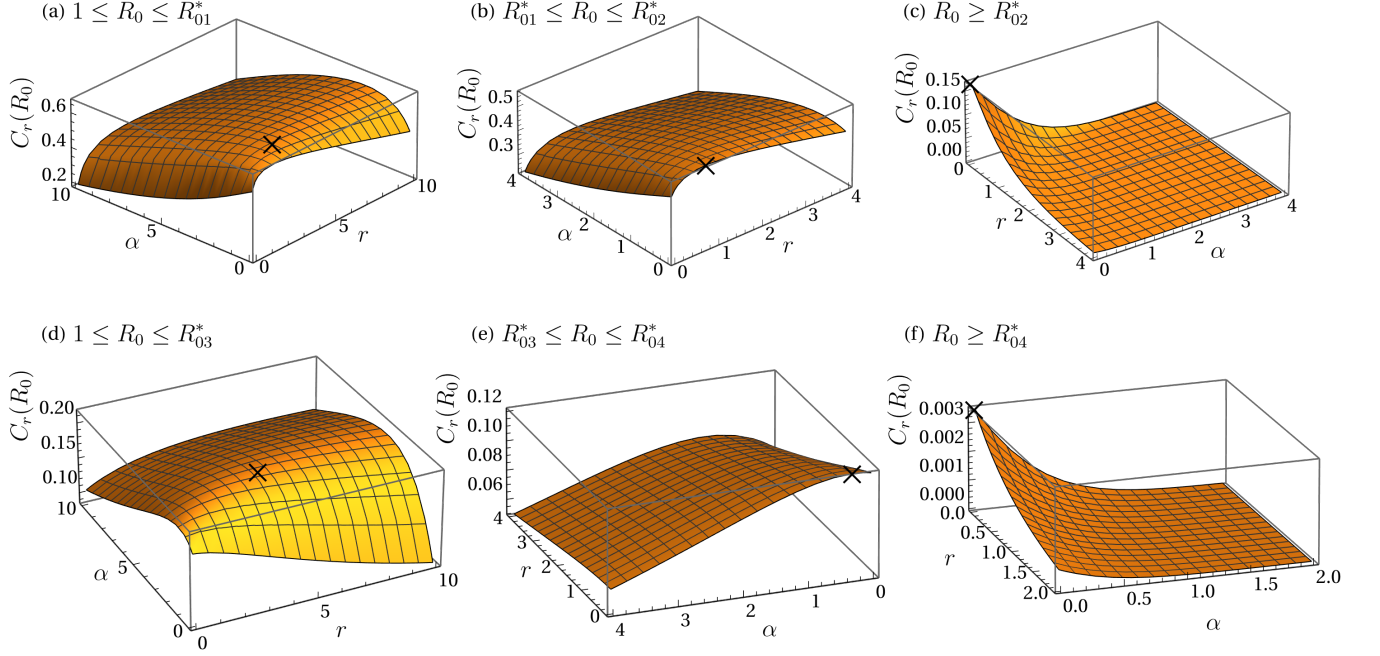


Figure 2. Three dimensional plots of the capture probability $C(R_0)$ in Eq. (10) as a function of (r, α) for different values of R_0 in one dimension. The cross denotes the maximum of $C(R_0)$ at the optimal values $(\bar{r}, \bar{\alpha})$. The top panels are for $b = 0.2 < b^* = 1.194933\dots$ while the bottom panels are for $b = 2 > b^*$. (a) $R_0 < R_{01}^*$ (b) $R_{01}^* < R_0 < R_{02}^*$ (c) $R_0 > R_{02}^*$ (d) $R_0 < R_{03}^*$ (e) $R_{03}^* < R_0 < R_{04}^*$ (f) $R_0 > R_{04}^*$. Note that in general R_{0i}^* for $i = 2, 3, 4$ are non-trivial functions of b (see Fig. 3 for exact values corresponding to $b = 0.2$ and $b = 2$).

time of this strategy. For convenience, we will express all length and time scales in units of some microscopic length and time units, i.e., space and time are rendered dimensionless.

To compute $C(\vec{R}_0)$ we proceed as follows. Let $Q_r(\vec{R}_0, t)$ denote the survival probability of the target up to time t , that is the probability that the target is not yet detected up to t . Then $[-\partial_t Q_r(\vec{R}_0, t)]$ is the first-passage probability, i.e., the capture probability at time t . The probability of survival of the strategy up to time t is simply $q(t) = \int_t^\infty p(\tau) d\tau = \int_t^\infty b e^{-b\tau} d\tau = e^{-bt}$. Hence the capture probability within this strategy is given by

$$C(\vec{R}_0) = \int_0^\infty dt \left[-\partial_t Q_r(\vec{R}_0, t) \right] e^{-bt}. \quad (1)$$

Performing integration by parts and using $Q_r(\vec{R}_0, 0) = 1$ one gets

$$C(\vec{R}_0) = \left[1 - b \tilde{Q}_r(\vec{R}_0, b) \right], \quad (2)$$

where $\tilde{Q}_r(\vec{R}_0, s) = \int_0^\infty Q_r(\vec{R}_0, t) e^{-st} dt$ is the Laplace transform of the survival probability. The survival probability (rather its Laplace transform) $\tilde{Q}_r(\vec{R}_0, s)$ in the presence of resetting can be related to the same quantity $\tilde{Q}_0(\vec{R}_0, s)$ in the absence of resetting via the well known

renewal relation [27, 45, 46]

$$\tilde{Q}_r(\vec{R}_0, s) = \frac{\tilde{Q}_0(\vec{R}_0, r + s)}{1 - r \tilde{Q}_0(\vec{R}_0, r + s)}. \quad (3)$$

Substituting Eq. (3) into Eq. (2) gives

$$C(\vec{R}_0) = \left[\frac{1 - (r + b) \tilde{Q}_0(\vec{R}_0, r + b)}{1 - r \tilde{Q}_0(\vec{R}_0, r + b)} \right]. \quad (4)$$

The survival probability $Q_0(\vec{R}_0, t)$, in the absence of resetting, satisfies the backward Fokker-Planck equation (see Supplemental Materials (SM) [47])

$$\frac{\partial Q_0(\vec{R}_0, t)}{\partial t} = D(R_0) \nabla^2 Q_0(\vec{R}_0, t) \quad (5)$$

with the initial condition $Q_0(\vec{R}_0, t = 0) = 1$ for all $R_0 > \epsilon$. The boundary condition is absorbing at $R_0 = \epsilon$, i.e., $Q_0(R_0 = \epsilon, t) = 0$ and also far from the target $Q_0(R_0 \rightarrow +\infty, t)$ remains finite. Since $D(R_0)$ depends only on the radial distance R_0 , the survival probability $Q_0(\vec{R}_0, t) = Q_0(R_0, t)$ also has spherical symmetry. Consequently, Eq. (5) becomes

$$\frac{\partial Q_0}{\partial t} = D(R_0) \left[\frac{\partial^2 Q_0}{\partial R_0^2} + \frac{d-1}{R_0} \frac{\partial Q_0}{\partial R_0} \right]. \quad (6)$$

From this backward Fokker-Planck equation one can read off the associated Langevin equation for the evolution of the radial coordinate $R(t)$

$$\frac{dR}{dt} = \frac{d-1}{R}D(R) + \sqrt{2D(R)}\eta(t) \quad (7)$$

where $\eta(t)$ is Gaussian white noise with zero mean and correlator $\langle \eta(t)\eta(t') \rangle = \delta(t-t')$ and the noise term has to be interpreted in the Itô sense since $D(R(t)) \equiv D(R)$ depends only on the instantaneous position at time t . When $D(R)$ is a constant independent of R , Eq. (7) just represents the well known Bessel process [48]. Such Langevin dynamics with multiplicative noise has also been widely studied in the context of the dynamics of subdiffusion in heterogeneous media [49–62].

To make further analytical progress, we need to specify a form of $D(R_0)$ in Eq. (6). Here, for simplicity, we focus on a specific family of non-increasing hopping rates, namely $D(R) = R^{-\alpha}$ with $\alpha \geq 0$. This is a very natural family of hopping rates with a single parameter α . This model has been studied in the context of transport in one dimensional inhomogeneous systems [52] and several statistical properties have been computed [56]. For this choice of $D(R_0)$, the survival probability $Q_0(R_0, t)$ can be obtained by solving Eq. (6). Taking the Laplace transform of Eq. (6) with respect to t , it is easy to show that (see SM [47]),

$$\tilde{Q}_0(R_0, s) = \frac{1}{s} \left[1 - \left(\frac{R_0}{\epsilon} \right)^{\frac{2-d}{2}} \frac{K_{(d-2)\mu} \left(2\mu\sqrt{s}R_0^{\frac{1}{2\mu}} \right)}{K_{(d-2)\mu} \left(2\mu\sqrt{s\epsilon^{\frac{1}{2\mu}}} \right)} \right] \quad (8)$$

where $\mu = 1/(\alpha + 2)$, $K_\nu(x)$ is the modified Bessel function of the second kind, and we recall that ϵ is the size of the target. Substituting Eq. (8) in Eq. (4) gives the exact capture probability $C(\vec{R}_0) \equiv C(R_0)$ as

$$C(R_0) = \frac{(b+r)}{r+b \left(\frac{R_0}{\epsilon} \right)^{\frac{d-2}{2}} \frac{K_{(d-2)\mu}(2\mu\sqrt{r+b}\epsilon^{1/2\mu})}{K_{(d-2)\mu}(2\mu\sqrt{r+b}R_0^{1/2\mu})}}. \quad (9)$$

This is one of our principal analytical results. As in the standard Brownian diffusion (the case $\alpha = 0$), it turns out for any $\alpha > 0$, the size ϵ of the target can be made as small as possible in $d < 2$, while for $d \geq 2$, one needs to keep a finite nonzero ϵ . This is because the trajectory will always miss, with probability 1, a point target for $d \geq 2$ [63, 64]. For example, in $d = 1$ upon taking the $\epsilon \rightarrow 0$ limit Eq. (9) simplifies to

$$C(R_0) = \frac{b+r}{r + \frac{b\Gamma(\mu)}{2\sqrt{R_0}\mu^\mu (r+b)^{\frac{1}{2\mu}} K_\mu \left(2\mu\sqrt{r+b}R_0^{\frac{1}{2\mu}} \right)}} \quad (10)$$

where we recall that $\mu = 1/(2 + \alpha)$. In Fig. 2 we plot $C(R_0)$ in Eq. (10) in the (r, α) plane. Fig. 2 clearly demonstrates that there is a unique global maximum of

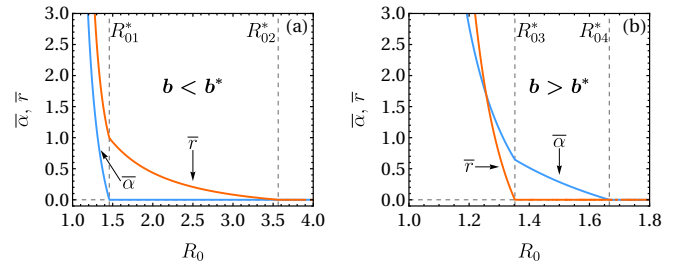


Figure 3. Plot of $\bar{\alpha}$ and \bar{r} , as a function of R_0 for (a) $b < b^* = 1.19494\dots$ and (b) $b > b^*$, in one dimension, obtained by maximizing Eq. (10). For both cases, \bar{r} and $\bar{\alpha}$ are nonanalytic at some critical values of R_0 (see SM [47]) marked by the vertical dash lines. For panel (a) we choose $b = 0.2 < b^*$, for which the critical values are at $R_{01}^* = 1.4578\dots$ and $R_{02}^* = 3.5634\dots$. For (b), we choose $b = 2 > b^*$, for which the critical values of R_0 are at $R_{03}^* = 1.35216\dots$ and $R_{04}^* = 1.6661\dots$.

$C(R_0)$ at an optimal value $(\bar{r}, \bar{\alpha})$. The same feature holds in higher dimensions as well. For example, in the End Matter we display similar figures for $d = 2$ (Fig. EM1) and $d = 3$ (Fig. EM3).

Hence, for fixed R_0 , ϵ and b we can optimize $C(R_0)$ in Eq. (9) in (r, α) plane and find the optimal parameters $(\bar{r}, \bar{\alpha})$. It is simpler to carry out this optimization in $d = 1$ (and $\epsilon \rightarrow 0$ limit) where we can use Eq. (10). Our analysis demonstrates rather interesting and rich phase transitions in these optimal values $(\bar{r}, \bar{\alpha})$ as one tunes R_0 and b . We now summarize these results. The optimal values $(\bar{r}, \bar{\alpha})$, as functions of R_0 and for fixed b , undergo a phase transition at two critical values of R_0 . However, the nature of the phases depends on b . It turns out that there is a threshold value b^* , across which two different scenarios emerge:

1. For $b < b^*$, we denote the two critical values as R_{01}^* and R_{02}^* . For $R_0 > R_{02}^*$, the optimal strategy corresponds to standard diffusion *without* resetting, i.e., $\bar{r} = 0$ and $\bar{\alpha} = 0$. For $R_{01}^* < R_0 < R_{02}^*$, the optimal strategy is standard diffusion *with* stochastic resetting [24, 25], i.e., $\bar{r} > 0$ and $\bar{\alpha} = 0$. Finally, for $R_0 < R_{01}^*$, the optimal strategy has both $\bar{r} > 0$ and $\bar{\alpha} > 0$.
2. For $b > b^*$, we denote the two critical values of R_0 by R_{03}^* and R_{04}^* . In this case, again $\bar{r} = 0$ and $\bar{\alpha} = 0$ for $R_0 > R_{04}^*$ and both $\bar{r} > 0$ and $\bar{\alpha} > 0$ for $R_0 < R_{03}^*$. In contrast to the $b < b^*$ case, here, for $R_{03}^* < R_0 < R_{04}^*$, we have $\bar{r}(R_0) = 0$ and $\bar{\alpha} > 0$.

This is illustrated in Fig. 3 for $d = 1$. However, these transitions turn out to be robust and generic and are also present in higher dimensions. We demonstrate this for $d = 2$ (see Fig. EM2) and $d = 3$ (see Fig. EM4). This nontrivial phase transition in the optimal parameters as functions of the initial distance R_0 (for a fixed target size ϵ) is our second main result. We also note that, as $R_0 \rightarrow 1^+$, for any b , both the optimal parameters diverge

as (see SM [47])

$$\bar{r} \approx \frac{9}{16e(R_0 - 1)^2} \quad \text{and} \quad \bar{\alpha} \approx \frac{1}{(R_0 - 1)} \quad (11)$$

where $e = \exp(1)$. Remarkably, Eq. (11) is universal at the leading order for all dimensions, and is independent of the target size ϵ . For $R_0 \leq 1$, the optimal pair of values freeze to $\bar{r} = +\infty$ and $\bar{\alpha} = +\infty$, and one can show that the optimized capture probability converges to unity.

In summary, we have studied search processes in situations where only partial information, namely, the distance to the target but not the direction is available to the searcher. We have introduced the *proxitaxis* search strategy and demonstrated that it can be made efficient in all dimensions by choosing an appropriate set of optimal parameters of this strategy. Our results demonstrate a very rich behavior, exhibiting multiple phase transitions in the optimal parameters in all dimensions. There are many directions in which the *proxitaxis* strategy can be

generalized, e.g., when there are multiple targets [65, 66] and/or when there are multiple searchers [67, 68].

To conclude, *proxitaxis* is a simple, analytically tractable, and efficient search strategy in the absence of any orientational information about the target. We hope that our results will stimulate interest in comparing real life animal movement data with our predictions. Furthermore, even if natural animals do not exactly follow this strategy, it can still be very useful for designing artificial search robots operating in situations where there is no orientational information available.

Acknowledgements.– We thank D. Boyer, L. Giuggioli and V. Krishnamurthy for providing us interesting references. We acknowledge support from the Science and Engineering Research Board (SERB, Government of India), under the VAJRA faculty scheme (VJR/2017/000110 and VJR/2019/00007). M. K. acknowledges support from the Department of Atomic Energy, Government of India, under project no. RTI4001. G. D. V. D. V. and S. N. M. acknowledge support from ANR Grant No. ANR-23-CE30-0020-01 EDIPS.

-
- [1] H. C. Berg and E. M. Purcell, *Biophys. J.* **20**, 193 (1977).
 [2] W. J. Bell, *Searching behaviour : the behavioural ecology of finding resources..* (Chapman & Hall, London, 1991).
 [3] J. M. Wolfe and T. S. Horowitz, *Nat Rev Neurosci* **5**, 495 (2004).
 [4] M. G. E. da Luz, A. Grosberg, E. P. Raposo, and G. M. Viswanathan, *J. Phys. A: Math. Theor.* **42**, 430301 (2009).
 [5] S. Andradóttir, A review of random search methods, in *Handbook of Simulation Optimization*, edited by M. C. Fu (Springer New York, New York, NY, 2015) pp. 277–292.
 [6] D. Grebenkov, R. Metzler, and G. Oshanin, in *Target Search Problems* (Springer, 2024).
 [7] M. Vergassola, E. Villermaux, and B. I. Shraiman, *Nature* **445**, 406 (2007).
 [8] A. Loisy and C. Eloy, *Proc. R. Soc. A.* **478**, 20220118 (2022).
 [9] C. Song, Y. He, B. Ristic, and X. Lei, *Rob. Auton. Syst.* **125**, 103414 (2020).
 [10] E. Martin Moraud and D. Martinez, *Front. Neurobot.* **4** (2010).
 [11] J. Adler, *Science* **153**, 708 (1966).
 [12] E. F. Keller and L. A. Segel, *J. Theor. Biol.* **30**, 225 (1971).
 [13] T. Payne, M. Birch, and C. Kennedy, *Mechanisms in Insect Olfaction*, Oxford science publications (Clarendon Press, 1986).
 [14] V. Sourjik and N. S. Wingreen, *Curr. Opin. Cell Biol.* **24**, 262 (2012).
 [15] D. Dusenbery and P. Dusenbery, *Sensory Ecology: How Organisms Acquire and Respond to Information* (W.H. Freeman, 1992).
 [16] J. Murlis, J. S. Elkinton, and R. T. Cardé, *Annu. Rev. Entomol.* **37**, 505 (1992).
 [17] H. Berg, *E. Coli in Motion* (Springer, 2014).
 [18] R. M. Holdo, R. D. Holt, and J. M. Fryxell, *The American Naturalist* **173**, 431 (2009).
 [19] W. F. Fagan, E. Gurarie, S. Bewick, A. Howard, R. S. Cantrell, and C. Cosner, *Am. Natl.* **189**, 474 (2017).
 [20] O. Bénichou, M. Coppey, M. Moreau, P.-H. Suet, and R. Voituriez, *Phys. Rev. Lett.* **94**, 198101 (2005).
 [21] M. A. Lomholt, K. Tal, R. Metzler, and K. Joseph, *Proc. Natl. Acad. Sci. U.S.A.* **105**, 11055 (2008).
 [22] O. Bénichou, M. Moreau, P.-H. Suet, and R. Voituriez, *J. Chem. Phys.* **126**, 234109 (2007).
 [23] O. Bénichou, C. Loverdo, M. Moreau, and R. Voituriez, *Rev. Mod. Phys.* **83**, 81 (2011).
 [24] M. R. Evans and S. N. Majumdar, *Phys. Rev. Lett.* **106**, 160601 (2011).
 [25] M. R. Evans and S. N. Majumdar, *J. Phys. A: Math. Theor.* **44**, 435001 (2011).
 [26] M. R. Evans and S. N. Majumdar, *J. Phys. A: Math. Theor.* **47**, 285001 (2014).
 [27] M. R. Evans, S. N. Majumdar, and G. Schehr, *J. Phys. A: Math. Theor.* **53**, 193001 (2020).
 [28] A. Pal, S. Kostinski, and S. Reuveni, *J. Phys. A: Math. Theor.* **55**, 021001 (2022).
 [29] S. Gupta and A. M. Jayannavar, *Front. Phys.* **10** (2022).
 [30] A. Kundu and S. Reuveni, *J. Phys. A: Math. Theor.* **57**, 060301 (2024).
 [31] P. C. Bressloff, *J. Phys. A: Math. Theor.* **53**, 105001 (2020).
 [32] M. R. Evans, S. N. Majumdar, and K. Mallick, *J. Phys. A: Math. Theor.* **46**, 185001 (2013).
 [33] S. Reuveni, *Phys. Rev. Lett.* **116**, 170601 (2016).
 [34] A. Pal and S. Reuveni, *Phys. Rev. Lett.* **118**, 030603 (2017).
 [35] A. Pal and V. V. Prasad, *Phys. Rev. E* **99**, 032123 (2019).
 [36] B. Besga, A. Bovon, A. Petrosyan, S. N. Majumdar, and S. Ciliberto, *Phys. Rev. Res.* **2**, 032029 (2020).
 [37] O. Tal-Friedman, A. Pal, A. Sekhon, S. Reuveni, and Y. Roichman, *J. Phys. Chem. Lett* **11**, 7350 (2020).
 [38] F. Faisant, B. Besga, A. Petrosyan, S. Ciliberto, and S. N.

- Majumdar, *J. Stat. Mech.* , 113203.
- [39] G. H. Pyke, H. R. Pulliam, and E. L. Charnov, *Q. Rev. Biol.* **52**, 137 (1977).
- [40] G. M. Viswanathan, M. G. E. da Luz, E. P. Raposo, and H. E. Stanley, *The Physics of Foraging: An Introduction to Random Searches and Biological Encounters* (Cambridge University Press, 2011).
- [41] G. Viswanathan, E. Raposo, and M. da Luz, *Phys. Life Rev.* **5**, 133 (2008).
- [42] T. Gueudré, A. Dobrinevski, and J.-P. Bouchaud, *Phys. Rev. Lett.* **112**, 050602 (2014).
- [43] M. Chupeau, O. Bénichou, and S. Redner, *Phys. Rev. E* **95**, 012157 (2017).
- [44] A. M. Hein, F. Carrara, D. R. Brumley, R. Stocker, and S. A. Levin, *Proc. Natl. Acad. Sci.* **113**, 9413 (2016).
- [45] L. Kusmierz, S. N. Majumdar, S. Sabhapandit, and G. Schehr, *Phys. Rev. Lett.* **113**, 220602 (2014).
- [46] S. Reuveni, *Phys. Rev. Lett.* **116**, 170601 (2016).
- [47] See Supplemental Materials.
- [48] D. Revuz and M. Yor, *Continuous martingales and Brownian motion*, Vol. 293 (Springer Science & Business Media, 2013).
- [49] K. S. Fa and E. K. Lenzi, *Phys. Rev. E* **67**, 061105 (2003).
- [50] A. G. Cherstvy, A. V. Chechkin, and R. Metzler, *New J. Phys.* **15**, 083039 (2013).
- [51] M. Lenzi, E. Lenzi, L. Guilherme, L. Evangelista, and H. Ribeiro, *Physica A* **588**, 126560 (2022).
- [52] A. Zodage, R. J. Allen, M. R. Evans, and S. N. Majumdar, *J. Stat. Mech.* , 033211 (2023).
- [53] A. L. Stella, A. Chechkin, and G. Teza, *Phys. Rev. Lett.* **130**, 207104 (2023).
- [54] A. L. Stella, A. Chechkin, and G. Teza, *Phys. Rev. E* **107**, 054118 (2023).
- [55] L. Menon and C. Anteneodo, *Phys. Rev. E* **110**, 054111 (2024).
- [56] G. Del Vecchio Del Vecchio and S. N. Majumdar, *J. Stat. Mech.* , 023207 (2025).
- [57] J. Eisinger, J. Flores, and W. Petersen, *Biophys. J.* **49**, 987 (1986).
- [58] M. Saxton, *Biophys. J.* **52**, 989 (1987).
- [59] M. Saxton, *Biophys. J.* **56**, 615 (1989).
- [60] M. Saxton, *Biophys. J.* **64**, 1766 (1993).
- [61] D. V. J. Nicolau, J. F. Hancock, and K. Burrage, *Biophys. J.* **92**, 1975 (2007).
- [62] H. Masuhara, S. Kawata, and F. Tokunaga, *Nano Biophotonics: Science and Technology* **3**, 175 (2007).
- [63] S. Redner, *A Guide to First-Passage Processes* (Cambridge University Press, 2001).
- [64] A. J. Bray, S. N. Majumdar, and G. Schehr, *Adv. Phys.* **62**, 225 (2013).
- [65] P. C. Bressloff, *Phys. Rev. E* **102**, 022115 (2020).
- [66] G. R. Calvert and M. R. Evans, *Eur. Phys. J. B* **94**, 228 (2021).
- [67] U. Bhat, C. De Bacco, and S. Redner, *J. Stat. Mech.* , 083401 (2016).
- [68] M. Biroli, S. N. Majumdar, and G. Schehr, *Phys. Rev. E* **107**, 064141 (2023).

End Matter

Optimization of the capture probability in two dimensions.— We discuss the capture probability in the case of $d = 2$. In this case the capture probability given in Eq. (9) becomes

$$C(R_0) = \frac{(b+r)}{r+b \frac{K_0(2\mu\sqrt{r+b}\epsilon^{1/2\mu})}{K_0(2\mu\sqrt{r+b}R_0^{1/2\mu})}}, \quad (\text{EM1})$$

where we recall that $\mu = 1/(2 + \alpha)$ and ϵ is the size of the object. We plot $C(R_0)$ given in Eq. (EM1) in the (r, α) plane in Fig. EM1 and see that for any fixed R_0 , there is indeed a unique global maximum at $(\bar{r}, \bar{\alpha})$. These optimal parameters undergo a phase transition at two critical values of R_0 as demonstrated in Fig. EM2.

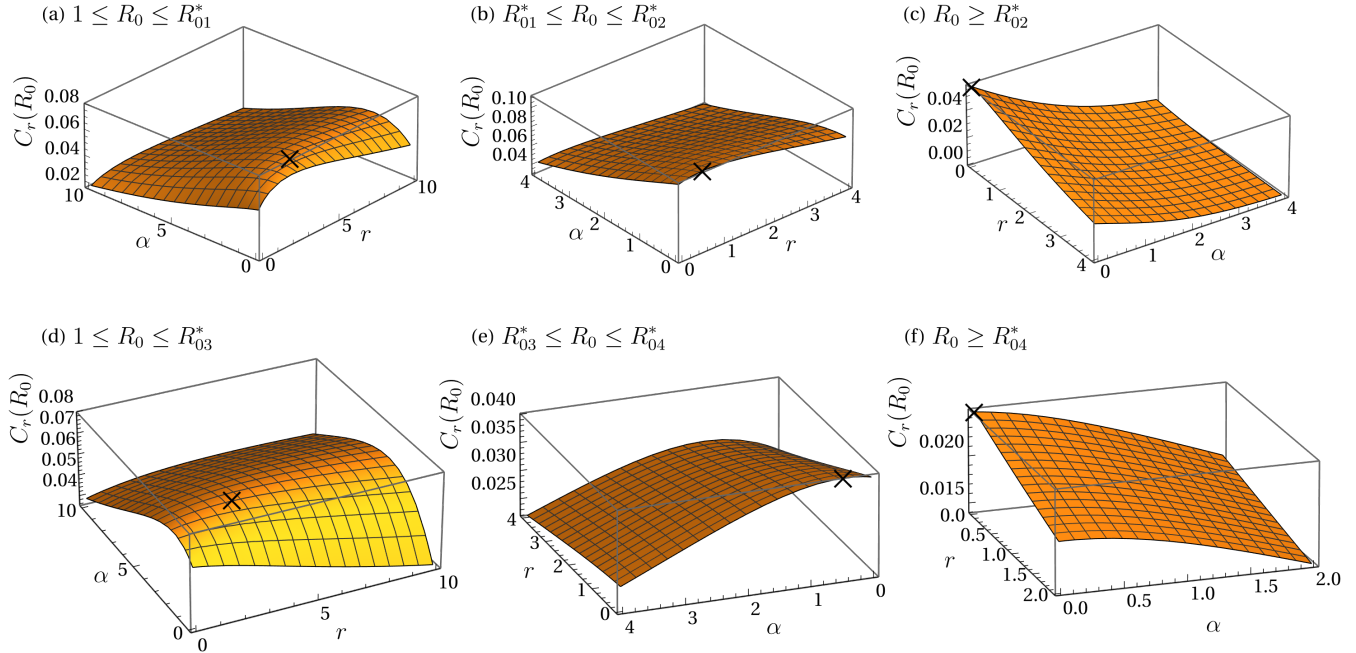


Figure EM1. Three dimensional plots of the capture probability $C(R_0)$ in Eq. (10) as a function of (r, α) for different values of R_0 in two dimensions $d = 2$ and target size $\epsilon = 0.2$. The cross denotes the maximum of $C(R_0)$ at the optimal values $(\bar{\alpha}, \bar{r})$. The top panels are for $b = 1 < b^*$ while the bottom panels are for $b = 4 > b^*$. (a) $R_0 < R_{01}^*$ (b) $R_{01}^* < R_0 < R_{02}^*$ (c) $R_0 > R_{02}^*$ (d) $R_0 < R_{03}^*$ (e) $R_{03}^* < R_0 < R_{04}^*$ (f) $R_0 > R_{04}^*$. Note that in general R_{0i}^* for $i = 2, 3, 4$ are non-trivial functions of b (see Fig. EM2 for exact values corresponding to $b = 1$ and $b = 4$).

Optimization of the capture probability in three dimensions.— For the $d = 3$ case, the capture probability given in Eq. (9) becomes

$$C(R_0) = \frac{(b+r)}{r+b \left(\frac{R_0}{\epsilon}\right)^{\frac{1}{2}} \frac{K_\mu(2\mu\sqrt{r+b}\epsilon^{1/2\mu})}{K_\mu(2\mu\sqrt{r+b}R_0^{1/2\mu})}}, \quad (\text{EM2})$$

where we recall that $\mu = 1/(2 + \alpha)$ and ϵ is the size of the target. Here again, we plot $C(R_0)$ given in Eq. (EM2) in the (r, α) plane in Fig. EM3 and see that for any fixed R_0 , there is indeed a unique global maximum at $(\bar{r}, \bar{\alpha})$. Similar to the one and two dimensional cases, these optimal parameters undergo a phase transition at two critical values of R_0 as demonstrated in Fig. EM4.

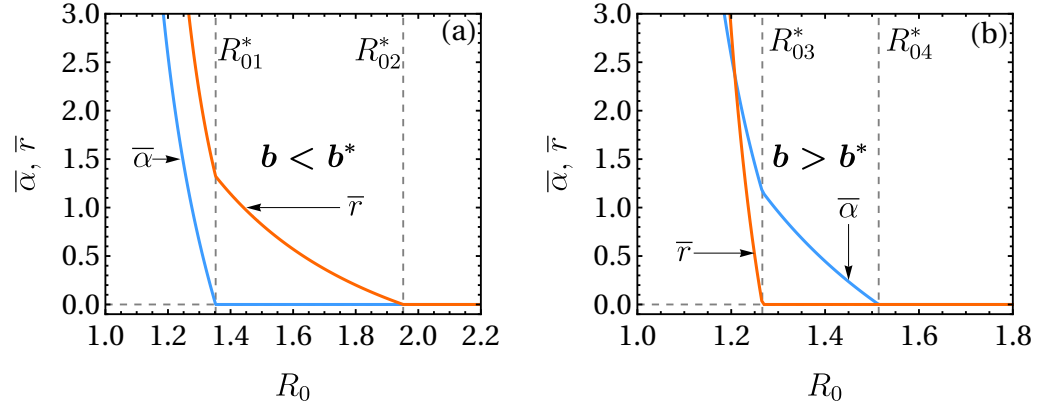


Figure EM2. Plot of \bar{r} and $\bar{\alpha}$, as a function of R_0 for (a) $b < b^*$ and (b) $b > b^*$, in two dimensions $d = 2$ and target size $\epsilon = 0.2$, obtained by maximizing Eq. (10). For both cases, \bar{r} and $\bar{\alpha}$ are nonanalytic at some critical values of R_0 (see SM [47]) marked by the vertical dash lines. For panel (a) we choose $b = 1 < b^*$, for which the critical values are at $R_{01}^* \approx 1.3524$ and $R_{02}^* \approx 1.9518$. For (b), we choose $b = 4 > b^*$, for which the critical values of R_0 are at $R_{03}^* \approx 1.2663$ and $R_{04}^* \approx 1.5142$.

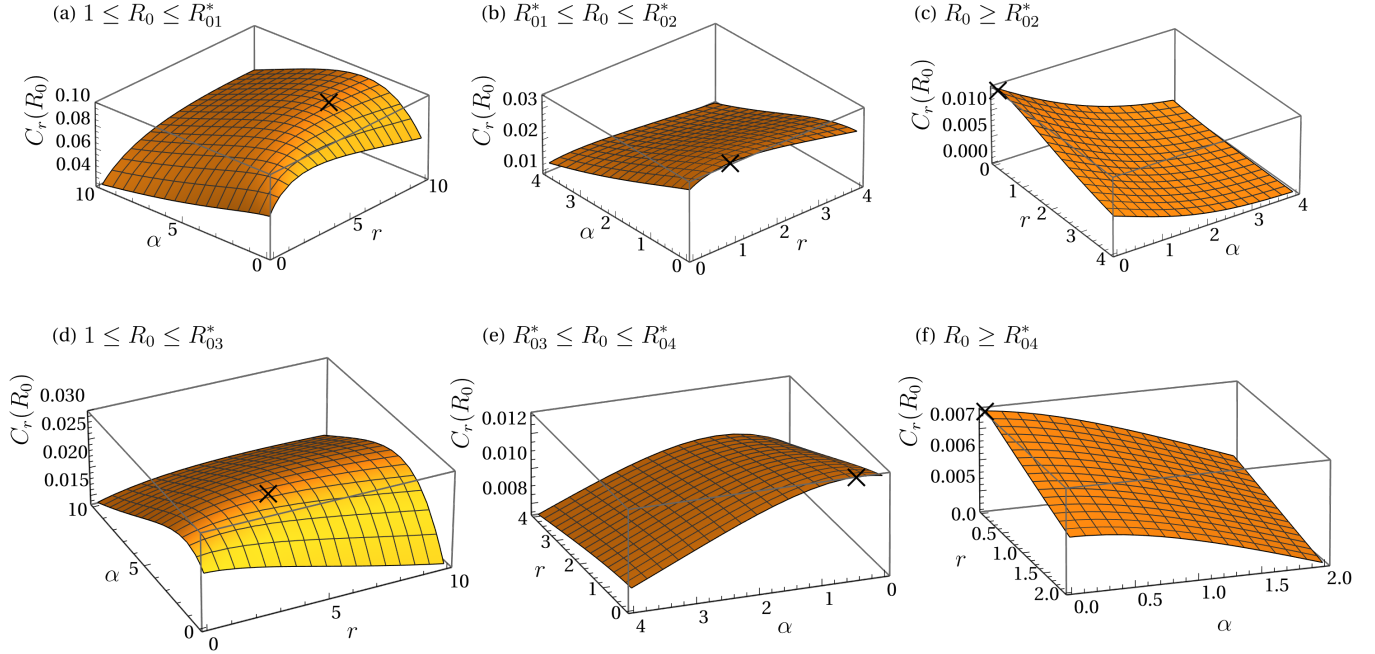


Figure EM3. Three dimensional plots of the capture probability $C(R_0)$ in Eq. (10) as a function of (r, α) for different values of R_0 in two dimensions $d = 3$ and target size $\epsilon = 0.2$. The cross denotes the maximum of $C(R_0)$ at the optimal values $(\bar{\alpha}, \bar{r})$. The top panels are for $b = 1 < b^*$ while the bottom panels are for $b = 4 > b^*$. (a) $R_0 < R_{01}^*$ (b) $R_{01}^* < R_0 < R_{02}^*$ (c) $R_0 > R_{02}^*$ (d) $R_0 < R_{03}^*$ (e) $R_{03}^* < R_0 < R_{04}^*$ (f) $R_0 > R_{04}^*$. Note that in general R_{0i}^* for $i = 2, 3, 4$ are non-trivial functions of b (see Fig. EM2 for exact values corresponding to $b = 1$ and $b = 4$).

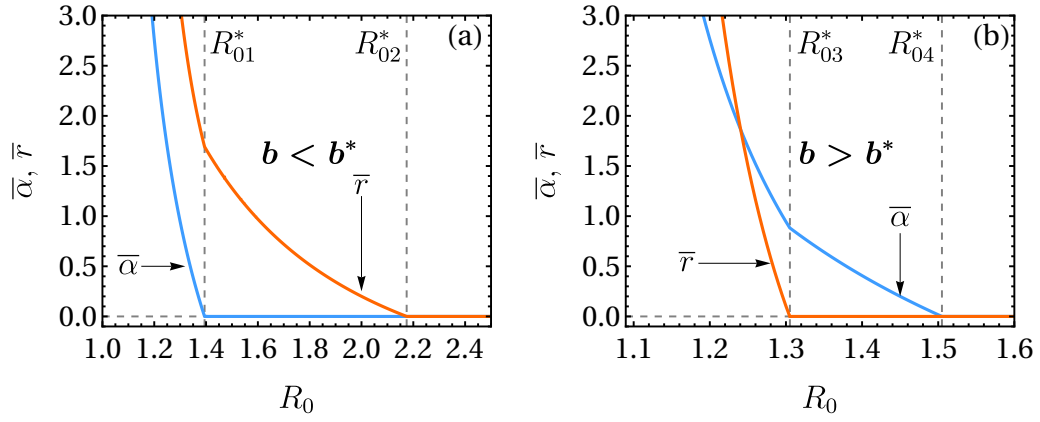


Figure EM4. Plot of \bar{r} and $\bar{\alpha}$, as a function of R_0 for (a) $b < b^*$ and (b) $b > b^*$, in three dimensions $d = 3$ and target size $\epsilon = 0.2$, obtained by maximizing Eq. (10). For both cases, \bar{r} and $\bar{\alpha}$ are nonanalytic at some critical values of R_0 (see SM [47]) marked by the vertical dash lines. For panel (a) we choose $b = 1 < b^*$, for which the critical values are at $R_{01}^* \approx 1.3943$ and $R_{02}^* \approx 2.1743$. For (b), we choose $b = 4 > b^*$, for which the critical values of R_0 are at $R_{03}^* \approx 1.3052$ and $R_{04}^* \approx 1.5049$.

Supplementary Material

CONTENTS

I. Details for the derivation of survival probability	10
II. Relation between the capture probability and the mean first passage time	11
III. Universal power-law divergence of the optimal parameters as $R_0 \rightarrow 1^+$	12
A. $d = 1$ case	12
B. $d = 2$ case	13
C. General $d > 2$ case	15
IV. Capture probability in the presence of a finite lifetime resetting strategy	16
References	18

I. DETAILS FOR THE DERIVATION OF SURVIVAL PROBABILITY

In this section, we discuss how to derive (8) of the main text. This quantity has been studied for $d = \alpha = 1$ in [1] and generalized to all $\alpha \in [0, +\infty)$ in [2] via a scaling argument. Here, we further generalize those results to arbitrary $\alpha \in [0, +\infty]$ and arbitrary dimensions d . The use of the backward Fokker-Planck approach is motivated by the fact that it directly gives access to $\tilde{Q}_0(R_0, s)$, i.e., the Laplace transform which is the main ingredient for the capture probability given in (4) of the main text.

We start from the Langevin equation Eq. (7) of the main text, which reads

$$\frac{dR}{dt} = \frac{d-1}{R}D(R) + \sqrt{2D(R)}\eta(t), \quad (\text{S1})$$

where the multiplicative white noise term is interpreted in the Itô sense. It is well known that the forward Fokker-Planck equation for the position probability distribution $P_0(R, t)$, in the absence of resetting, reads [1–5]

$$\frac{\partial P_0}{\partial t} = \frac{\partial^2}{\partial r^2} [D(R)P_0] - \frac{\partial}{\partial r} \left[\frac{d-1}{R}D(R)P_0 \right]. \quad (\text{S2})$$

In contrast, the survival probability $Q_0(R, t)$, where R_0 is the starting position, satisfies the backward Fokker-Planck equation (the adjoint of Eq. (S2))

$$\frac{\partial Q_0}{\partial t} = D(R_0) \left[\frac{\partial^2 Q_0}{\partial R_0^2} + \frac{d-1}{R_0} \frac{\partial Q_0}{\partial R_0} \right], \quad (\text{S3})$$

valid for $R_0 > \epsilon$. It satisfies the boundary

$$Q_0(R_0 = \epsilon, t) = 0 \quad \text{and} \quad Q_0(R_0 \rightarrow +\infty, t) = 1. \quad (\text{S4})$$

The first condition comes from the fact that when the boundary $R_0 = \epsilon$ is absorbing, i.e., if the particle starts from this boundary it does not survive up to any finite time t . The second boundary condition comes from the fact that if the particle starts very far from the target it definitely survives up to any finite time t with probability 1. Eq. (S4) starts from the initial condition

$$Q_0(R_0, 0) = 1 \quad \text{for all} \quad R_0 > \epsilon. \quad (\text{S5})$$

Here $0 < \epsilon < R_0$ is the radius of the finite-size target. To proceed, it is convenient to define the Laplace transform with respect to t as

$$\tilde{Q}_0(R_0, s) = \int_0^{+\infty} d\tau e^{-s\tau} Q_0(R_0, \tau). \quad (\text{S6})$$

Taking the Laplace transform of Eq. (S4) and with the choice $D(R) = r^{-\alpha}$ one gets

$$-1 + s\tilde{Q}_0 = \frac{1}{R_0^\alpha} \frac{\partial^2 \tilde{Q}_0}{\partial R_0^2} + \frac{d-1}{R_0^{\alpha+1}} \frac{\partial \tilde{Q}_0}{\partial R_0}. \quad (\text{S7})$$

Shifting \tilde{Q}_0 by $1/s$ and solving the result homogeneous equation one gets

$$\tilde{Q}_0(R_0, s) = A R_0^{\frac{2-d}{2}} K_{\mu(d-2)} \left(2\mu s^{\frac{1}{2}} R_0^{\frac{1}{2\mu}} \right) + B R_0^{\frac{2-d}{2}} I_{\mu(d-2)} \left(2\mu s^{\frac{1}{2}} R_0^{\frac{1}{2\mu}} \right) + \frac{1}{s}, \quad (\text{S8})$$

where A and B are constants and $I_\mu(x)$ and $K_\mu(x)$ are modified Bessel functions of the first and second kind respectively. From the known asymptotic behaviors of the modified Bessel functions [6]

$$K_\mu(x) \sim \sqrt{\pi/(2x)} e^{-x} \quad \text{and} \quad I_\nu(x) \sim \sqrt{\pi/(2x)} e^x \quad \text{as} \quad x \rightarrow +\infty, \quad (\text{S9})$$

we see that the first condition in Eq. (S4) imposes $B = 0$ because that term is divergent. To find the constant A , we impose the second boundary condition $\tilde{Q}(\epsilon, s) = 0$ in Eq. (S4). This gives

$$A = -\frac{1}{s} \frac{1}{\epsilon^{\frac{2-d}{2}} K_{\mu(d-2)} \left(2\mu s^{\frac{1}{2}} \epsilon^{\frac{1}{2\mu}} \right)}. \quad (\text{S10})$$

Substituting A from Eq. (S10) and $B = 0$ in Eq. (S8) gives

$$\tilde{Q}_0(R_0, s) = \frac{1}{s} \left[1 - \left(\frac{R_0}{\epsilon} \right)^{\frac{2-d}{2}} \frac{K_{(d-2)\mu} \left(2\mu \sqrt{s} R_0^{\frac{1}{2\mu}} \right)}{K_{(d-2)\mu} \left(2\mu \sqrt{s} \epsilon^{\frac{1}{2\mu}} \right)} \right], \quad (\text{S11})$$

which is Eq. (8) in the main text.

II. RELATION BETWEEN THE CAPTURE PROBABILITY AND THE MEAN FIRST PASSAGE TIME

In this section we establish an exact relation, in the presence of resetting, between the capture probability $C(R_0)$ and the mean first passage time (MFPT), denoted $T_r(R_0)$. Let $F_r(R_0, t)$ denote the first passage probability density to the target for a particle starting at R_0 and resetting to R_0 with rate r . Clearly [7, 8]

$$F_r(R_0, t) = -\frac{\partial Q_0(R_0, t)}{\partial t}. \quad (\text{S12})$$

Then the MFPT is just the first moment of the first passage probability density and it is given by

$$T_r(R_0) = \int_0^{+\infty} F_r(R_0, t) t dt = \int_0^{+\infty} [-\partial_t Q_r(R_0, t)] t dt. \quad (\text{S13})$$

Integrating by parts and using the initial condition given in Eq. (S5) gives

$$T_r(R_0) = \int_0^\infty Q_r(R_0, t) dt = \tilde{Q}_r(R_0, 0). \quad (\text{S14})$$

Next, we use the relation between the survival probability with and without resetting (as given in Eq. (3) of the main text)

$$\tilde{Q}_r(R_0, s) = \frac{\tilde{Q}_0(R_0, r+s)}{1 - r\tilde{Q}_0(R_0, r+s)} \quad (\text{S15})$$

in Eq. (S14) with $s = 0$. This gives

$$T_r(R_0) = \frac{\tilde{Q}_0(R_0, r)}{1 - r\tilde{Q}_0(R_0, r)}. \quad (\text{S16})$$

On the other hand the capture probability is given by (see Eq. (4) of the main text)

$$C(R_0) = \left[\frac{1 - (r+b) \tilde{Q}_0(R_0, r+b)}{1 - r \tilde{Q}_0(R_0, r+b)} \right]. \quad (\text{S17})$$

Now, it is easy to see that Eq. (S17) can be expressed in terms of $T_r(R_0)$ in Eq. (S16) as

$$C(R_0) = \frac{1}{1 + b T_{r+b}(R_0)}. \quad (\text{S18})$$

Therefore, maximizing the capture probability $C(R_0)$ with respect to the parameters (r, α) is equivalent to minimizing the MPFT $T_{r+b}(R_0)$ with respect to $(r+b, \alpha)$. Recall from the main text that in d dimensions (also see Sec. I for a derivation)

$$\tilde{Q}_0(R_0, s) = \frac{1}{s} \left[1 - \left(\frac{R_0}{\epsilon} \right)^{\frac{2-d}{2}} \frac{K_{(d-2)\mu} \left(2\mu\sqrt{s} R_0^{\frac{1}{2\mu}} \right)}{K_{(d-2)\mu} \left(2\mu\sqrt{s\epsilon} \frac{1}{2\mu} \right)} \right], \quad (\text{S19})$$

where $\mu = 1/(\alpha + 2)$, $K_\nu(x)$ is the modified Bessel function of the second kind, and ϵ is the size of the target. Using Eq. (S19) in Eq. (S16), we get

$$T_r(R_0) = \frac{1}{r} \left[\left(\frac{R_0}{\epsilon} \right)^{(d-2)/2} \frac{K_{(d-2)\mu} \left(2\mu\sqrt{r\epsilon}^{1/2\mu} \right)}{K_{(d-2)\mu} \left(2\mu\sqrt{r} R_0^{1/2\mu} \right)} - 1 \right]. \quad (\text{S20})$$

III. UNIVERSAL POWER-LAW DIVERGENCE OF THE OPTIMAL PARAMETERS AS $R_0 \rightarrow 1^+$

A. $d = 1$ case

In (11) of the main text, we have reported the divergent behavior of \bar{r} and $\bar{\alpha}$ as the resetting distance R_0 from the target site approaches unity from above. Here, we provide a detailed derivation. Our results in Fig. 3 of the main text indicate that there is a divergence of \bar{r} and $\bar{\alpha}$ as $R_0 \rightarrow 1^+$. As mentioned in Sec. II, the problem of maximizing the capture probability $C(R_0)$ is equivalent to that of minimizing MPFT $T_{r+b}(R_0)$. It turns out that minimizing the MFPT is somehow easier than maximizing $C(R_0)$. In one dimension, using Eq. (S20), the MFPT is given by

$$T_{r+b}(R_0) = \frac{1}{r+b} \left[\frac{\Gamma(\mu)}{2z^\mu K_\mu(2z)} - 1 \right], \quad (\text{S21})$$

where we introduce a scaling variable

$$z = \mu\sqrt{r+b} R_0^{1/(2\mu)}. \quad (\text{S22})$$

Eq. (S22) naturally suggests that one should keep the combination $\mu\sqrt{r+b}$ fixed when taking limit $\alpha \rightarrow \infty$, i.e., $\mu \rightarrow 0$ and $(r+b) \rightarrow \infty$. Since we assume b is a constant $\sim O(1)$, $(r+b) \rightarrow \infty$ is equivalent to just $r \rightarrow \infty$. In this limit, $R_0^{1/(2\mu)} \rightarrow \infty$ for $R_0 > 1$. We then use the asymptotic behavior

$$K_\mu(2z) \sim \sqrt{\pi/(4z)} e^{-2z} \quad \text{as } z \rightarrow \infty. \quad (\text{S23})$$

Taking the limit $\mu \rightarrow 0$, $r \rightarrow \infty$ keeping $\mu\sqrt{r}$ fixed and setting $R_0 = 1 + \delta$ with $\delta > 0$ small, in Eq. (S21), we get [using Eq. (S23)]

$$T_r(R_0) \approx \frac{1}{r} \left[\frac{r^{1/4}}{\sqrt{\mu\pi}} e^{(\frac{1}{4\mu} - \frac{1}{2})\delta} e^{2\mu\sqrt{r} e^{\delta/(2\mu)}} - 1 \right]. \quad (\text{S24})$$

We recall that, since $b \sim O(1)$ we have replaced the combination $(r+b)$ merely with r everywhere. Taking derivatives of Eq. (S24) with respect to μ and r and equating them to zero yields

$$2\mu + 4\mu\sqrt{r} e^{\frac{\delta}{2\mu}} (\delta - 2\mu) + \delta = 0 \quad (\text{S25})$$

and

$$e^{\frac{\delta}{4\mu} + 2\mu\sqrt{r}} e^{\frac{\delta}{2\mu}} \left(4\mu\sqrt{r} e^{\frac{\delta}{2\mu}} - 3 \right) + 4\sqrt{\pi} r^{-1/4} \sqrt{\mu} e^{\delta/2} = 0 \quad (\text{S26})$$

respectively. Solving Eq. (S25) and Eq. (S26) gives the optimal r and μ as a function of δ where we recall that δ quantifies the proximity of R_0 to unity. To this end, it is convenient to express the solution of the ratio $w = \mu/\delta$ and δ . Equation (S25) then becomes

$$\sqrt{r} = \frac{1}{\delta} G\left(\frac{\mu}{\delta}\right), \quad \text{where} \quad G(w) = \frac{1}{4w} \left(\frac{2w+1}{2w-1} \right) e^{-\frac{1}{2w}}. \quad (\text{S27})$$

We next substitute the expression of \sqrt{r} from Eq. (S27) in Eq. (S26), which gives

$$f(w) = \delta e^{\delta/2} \quad \text{where} \quad f(w) = \sqrt{\frac{2w+1}{2w-1}} \frac{(w-1)}{(2w-1)} \frac{1}{2\sqrt{\pi}w} e^{\frac{2w+1}{2(2w-1)}}. \quad (\text{S28})$$

From Eq. (S28), when $\delta \rightarrow 0$, it is clear that $w \rightarrow 1$. Expanding $f(w)$ around $w = 1$ one gets to leading order,

$$f(w) \approx \frac{\sqrt{3}e^{3/2}}{2\sqrt{\pi}}(w-1). \quad (\text{S29})$$

Therefore, inverting the relation $f(w) = \delta$ gives the optimal value of w as

$$w = 1 + \frac{2\sqrt{\pi}}{\sqrt{3}e^{3/2}} \delta + O(\delta^2). \quad (\text{S30})$$

We recall that the optimal solutions for r and α are denoted by \bar{r} and $\bar{\alpha}$ respectively. Since $\mu = \delta w$, the optimal exponent $\bar{\mu} = 1/(\bar{\alpha} + 2)$ is given by

$$\frac{1}{\bar{\alpha} + 2} = \delta + O(\delta^2). \quad (\text{S31})$$

Consequently, to leading order in δ , one gets

$$\bar{\alpha} = \frac{1}{\delta} + O(1). \quad (\text{S32})$$

Similarly, one can express the optimal value \bar{r} in terms of δ as follows. Using the fact that when $\delta \rightarrow 0$, the ratio $w \rightarrow 1$. Hence, from Eq. (S27), one gets to leading order in δ ,

$$\bar{r} \approx \frac{1}{\delta^2} G^2(1) = \frac{9}{16e\delta^2}, \quad (\text{S33})$$

where $e = \exp(1.0)$. Hence, to summarize, to leading order in $\delta = R_0 - 1$, the optimal parameters $\{\bar{\alpha}, \bar{r}\}$ both diverge as

$$\bar{r} \approx \frac{9}{16e(R_0 - 1)^2} \quad \text{and} \quad \bar{\alpha} \approx \frac{1}{(R_0 - 1)}, \quad (\text{S34})$$

which is precisely (11) of the main text.

B. $d = 2$ case

In two dimensions, we again start with Eq. (S20) and substitute $d = 2$. For $\epsilon < 1$, taking the limit $\mu \rightarrow 0$, $r \rightarrow \infty$ keeping $\mu\sqrt{r}$ fixed and setting $R_0 = 1 + \delta$ with $\delta > 0$ small, we get

$$T_r(R_0) \approx \frac{1}{r} \left[- \left(\log(2\mu\sqrt{r}) + \frac{\ln \epsilon}{2\mu} \right) \frac{2\sqrt{\mu}r^{1/4}}{\sqrt{\pi}} \exp\left(\frac{\delta}{4\mu} + 2\mu\sqrt{r} \exp\left(\frac{\delta}{2\mu} \right) \right) - 1 \right]. \quad (\text{S35})$$

Taking a derivative of Eq. (S35) with respect to μ and setting it to zero gives

$$\left[2\mu + 4\mu\sqrt{r}e^{\frac{\delta}{2\mu}}(\delta - 2\mu) + \delta \right] \ln \epsilon = 8\mu^2 + \ln(2\mu\sqrt{r}) \left[4\mu^2 - 2\delta\mu - 8\mu\sqrt{r}e^{\frac{\delta}{2\mu}}(\delta - 2\mu)\mu \right]. \quad (\text{S36})$$

Similarly, taking a derivative of Eq. (S35) with respect to r and setting it to zero gives

$$4\sqrt{\pi}r^{-1/4}\sqrt{\mu} = e^{\frac{\delta}{4\mu} + 2\mu\sqrt{r}e^{\frac{\delta}{2\mu}}} \left[2\mu \left(\left[4\mu\sqrt{r}e^{\frac{\delta}{2\mu}} - 3 \right] \ln(2\mu\sqrt{r}) + 2 \right) + \left(4\mu\sqrt{r}e^{\frac{\delta}{2\mu}} - 3 \right) \ln \epsilon \right]. \quad (\text{S37})$$

Equations (S36) and (S37) together determines μ and r as a function of $\delta = R_0 - 1$. We are interested in their behavior as $\delta \rightarrow 0$. To this end, similar to the one dimensional case in Sec. III A, it is convenient to define the variable $w = \mu/\delta$. In the scaling limit $\delta \rightarrow 0$, $\mu \rightarrow 0$, and $r \rightarrow \infty$, keeping $\mu/\delta = w$ and $r\delta^2$ fixed, Eq. (S36) admits the scaling solution for r as

$$\sqrt{r} = \frac{1}{\delta} G\left(\frac{\mu}{\delta}\right), \quad \text{where} \quad G(w) = \frac{1}{4w} \left(\frac{2w+1}{2w-1} \right) e^{-\frac{1}{2w}}. \quad (\text{S38})$$

Interestingly, $G(z)$ in Eq. (S38), is exactly the same scaling function that also appears in Eq. (S27) in the $d = 1$ case [Sec. III A]. Using this scaling solution of r in Eq. (S37) together with setting $\mu = w\delta$, gives an equation that determines w in terms of δ . This equation turns out to be

$$f(w) = \frac{\delta}{(-\ln \epsilon)} g(w), \quad (\text{S39})$$

where

$$g(w) = 1 - \frac{e^{\frac{2w+1}{2(2w-1)}} \sqrt{2w+1}}{2\sqrt{\pi}w(2w-1)^{3/2}} \left[2w^2 - 1 - 2(w-1)w \ln \left(\frac{2w+1}{2(2w-1)} \right) \right], \quad (\text{S40})$$

and we recall that $f(w)$ in Eq. (S39) is the same function that appears in Eq. (S28). From Eq. (S39), it is clear that $w \rightarrow 1$ when $\delta \rightarrow 0$. Therefore, we expand Eq. (S39) around $w = 1$ to the leading order,

$$(w-1)f'(1) = \frac{\delta}{(-\ln \epsilon)} g(1) + O((w-1)^2). \quad (\text{S41})$$

This gives

$$w = 1 + \frac{\delta}{(-\ln \epsilon)} \frac{g(1)}{f'(1)} + O(\delta^2). \quad (\text{S42})$$

From Eq. (S39) and Eq. (S40), we get

$$f'(1) = \frac{\sqrt{3}e^{3/2}}{2\sqrt{\pi}} \quad \text{and} \quad g(1) = 1 - \frac{\sqrt{3}e^{3/2}}{2\sqrt{\pi}}. \quad (\text{S43})$$

Finally, substituting Eq. (S43) in Eq. (S42) we get

$$w = 1 + \left(1 - \frac{2\sqrt{\pi}}{\sqrt{3}e^{3/2}} \right) \frac{\delta}{\ln \epsilon} + O(\delta^2). \quad (\text{S44})$$

We recall that the optimal solutions for r and α are denoted by \bar{r} and $\bar{\alpha}$ respectively. Since $\mu = \delta w$, the optimal exponent $\bar{\mu} = 1/(\bar{\alpha} + 2)$ is given by

$$\frac{1}{\bar{\alpha} + 2} = \delta + O(\delta^2). \quad (\text{S45})$$

Consequently, to leading order in δ , one gets

$$\bar{\alpha} = \frac{1}{\delta} + O(1). \quad (\text{S46})$$

Similarly, one can express the optimal value \bar{r} in terms of δ as follows. Note from Eq. (S42) that when $\delta \rightarrow 0$, the ratio w approaches unity. Hence, from Eq. (S38), one gets to leading order in δ ,

$$\bar{r} \approx \frac{1}{\delta^2} G^2(1) = \frac{9}{16 e \delta^2}, \quad (\text{S47})$$

where $e = \exp(1.0)$. Hence, to summarize, to leading order in $\delta = R_0 - 1$, the optimal parameters $(\bar{r}, \bar{\alpha})$ both diverge as

$$\bar{\alpha} \approx \frac{1}{(R_0 - 1)} \quad \text{and} \quad \bar{r} \approx \frac{9}{16 e (R_0 - 1)^2}. \quad (\text{S48})$$

Thus, in $d = 2$, the leading order behavior of the optimal parameters $(\bar{r}, \bar{\alpha})$ as $R_0 \rightarrow 1^+$ is independent of ϵ . The ϵ -dependence comes only in the sub-leading orders. This makes the leading order result universal, i.e., same as in $d = 1$ [see Eq. (S34)].

C. General $d > 2$ case

For general $d > 2$, we again start with Eq. (S20). For $\epsilon < 1$, taking the limit $\mu \rightarrow 0$, $r \rightarrow \infty$ keeping $\mu\sqrt{r}$ fixed and setting $R_0 = 1 + \delta$ with $\delta > 0$ small, we get

$$T_r(R_0) \approx \frac{1}{r} \left[\frac{r^{1/4}}{|\gamma| \epsilon^{\frac{1}{2}(|\gamma|+\gamma)} \sqrt{\pi} \mu} e^{(\frac{1}{4\mu} + \frac{\gamma}{2})\delta + 2\mu\sqrt{r}e^{\frac{\delta}{2\mu}}} - 1 \right], \quad \text{where } \gamma = d - 2. \quad (\text{S49})$$

Taking a derivative of Eq. (S49) with respect to μ and equating it to zero we get

$$2\mu + 4\mu\sqrt{r}e^{\frac{\delta}{2\mu}}(\delta - 2\mu) + \delta = 0. \quad (\text{S50})$$

This is indeed exactly the same equation (S25) that we obtained for the $d = 1$ case that admits the exact scaling solution for r (for all δ) as [see Eq. (S27) for $d = 1$, and Eq. (S38) for $d = 2$ with $\delta \rightarrow 0$]

$$\sqrt{r} = \frac{1}{\delta} G\left(\frac{\mu}{\delta}\right), \quad \text{where } G(w) = \frac{1}{4w} \left(\frac{2w+1}{2w-1}\right) e^{-\frac{1}{2w}}. \quad (\text{S51})$$

Note that this is independent of the target size ϵ . Similar to both $d = 1$ (Sec III A) and $d = 2$ (Sec III B) case, taking a derivative of Eq. (S49) with respect to r ,

$$4\sqrt{\pi} |\gamma| \epsilon^{\frac{|\gamma|+\gamma}{2}} r^{-1/4} \sqrt{\mu} e^{-\gamma/2} + \left(4\mu\sqrt{r}e^{\frac{\delta}{2\mu}} - 3\right) e^{\frac{\delta}{4\mu} + 2\mu\sqrt{r}e^{\frac{\delta}{2\mu}}} = 0. \quad (\text{S52})$$

We next substitute the expression of \sqrt{r} from Eq. (S51) in Eq. (S52), which gives

$$f(w) = |\gamma| \epsilon^{\frac{|\gamma|+\gamma}{2}} \delta e^{-\gamma\delta/2}, \quad (\text{S53})$$

where $f(w)$ is given in Eq. (S28). Note that for $d = 1$, we have $\gamma = -1$. Hence, Eq. (S53) reproduces Eq. (S28) for $d = 1$. For general $d > 2$, from Eq. (S53), when $\delta \rightarrow 0$, we have $w \rightarrow 1$. Therefore, using the expansion of $f(w)$ near $w = 1$ from Eq. (S29), we get

$$w = 1 + \frac{2\sqrt{\pi}}{\sqrt{3}} e^{-3/2} |\gamma| \epsilon^{\frac{|\gamma|+\gamma}{2}} \delta + O(\delta^2). \quad (\text{S54})$$

We recall that the optimal solutions for r and α are denoted by \bar{r} and $\bar{\alpha}$ respectively. Since $\mu = \delta w$, the optimal exponent $\bar{\mu} = 1/(\bar{\alpha} + 2)$ is given by

$$\frac{1}{\bar{\alpha} + 2} = \delta + O(\delta^2). \quad (\text{S55})$$

Consequently, to leading order in δ , one gets

$$\bar{\alpha} = \frac{1}{\delta} + O(1). \quad (\text{S56})$$

Similarly, one can express the optimal value \bar{r} in terms of δ as follows. Using the fact that when $\delta \rightarrow 0$, the ratio $w \rightarrow 1$. Hence, from Eq. (S51), one gets to leading order in δ ,

$$\bar{r} \approx \frac{1}{\delta^2} G^2(1) = \frac{9}{16 e \delta^2}, \quad (\text{S57})$$

where $e = \exp(1.0)$. Hence, to summarize, to leading order in $\delta = R_0 - 1$, the optimal parameters $(\bar{r}, \bar{\alpha})$ both diverge as

$$\bar{r} \approx \frac{9}{16 e (R_0 - 1)^2} \quad \text{and} \quad \bar{\alpha} \approx \frac{1}{(R_0 - 1)}. \quad (\text{S58})$$

Thus, as in $d = 2$, we find that the leading order behaviors of \bar{r} and $\bar{\alpha}$ as $R_0 \rightarrow 1^+$ are independent of ϵ . Moreover, they are exactly the same for all $d > 2$ and $d = 1, 2$. Hence, the leading order behaviors of the optimal parameters \bar{r} and $\bar{\alpha}$ as $R_0 \rightarrow 1^+$ are universal in the sense that they do not depend on the dimension d .

IV. CAPTURE PROBABILITY IN THE PRESENCE OF A FINITE LIFETIME RESETTING STRATEGY

As reported in the main text in (4), the capture probability, $C(\bar{R}_0) \equiv C(R_0)$, is given by

$$C(R_0) = \left[\frac{1 - (r + b) \tilde{Q}_0(R_0, r + b)}{1 - r \tilde{Q}_0(R_0, r + b)} \right], \quad (\text{S59})$$

where the Laplace transform of the survival probability is given in Eq. (S11). This gives the exact expression of the capture probability within this strategy

$$C(R_0) = \frac{(b + r)}{r + b \left(\frac{R_0}{\epsilon}\right)^{(d-2)/2} \frac{K_{(d-2)\mu}(2\mu(r+b)^{1/2} \epsilon^{1/2\mu})}{K_{(d-2)\mu}(2\mu(r+b)^{1/2} R_0^{1/2\mu})}}. \quad (\text{S60})$$

Our goal now is to maximize the function $C(R_0)$ with respect to the two parameters (r, α) for fixed R_0, b and ϵ . It turns out that it is easier to work with the parameters (r, μ) [where $\mu = 1/(\alpha + 2)$] rather than with (r, α) . The optimal parameters $(\bar{r}, \bar{\mu})$ that maximize $C(R_0)$ can be obtained by solving simultaneously the pair of equations

$$\partial_r C(R_0) \Big|_{(\bar{r}, \bar{\mu})} = 0 \quad \text{and} \quad \partial_\mu C(R_0) \Big|_{(\bar{r}, \bar{\mu})} = 0. \quad (\text{S61})$$

Differentiating Eq. (S59) with respect to r , we get

$$\partial_r C(R_0) = -b \frac{\partial_r \tilde{Q}_0(R_0, r + b) + Q_0^2(R_0, r + b)}{[1 - r \tilde{Q}_0(R_0, r + b)]^2}. \quad (\text{S62})$$

Therefore, using Eq. (S62) in the first condition in Eq. (S61) gives

$$\left[\partial_r \tilde{Q}_0(R_0, r + b) + \tilde{Q}_0(R_0, r + b)^2 \right] \Big|_{(\bar{r}, \bar{\mu})} = 0. \quad (\text{S63})$$

Similarly, differentiating Eq. (S59) with respect to μ yields

$$\partial_\mu C(R_0) = -b \frac{\partial_\mu \tilde{Q}_0(R_0, r + b)}{[1 - r \tilde{Q}_0(R_0, r + b)]^2}. \quad (\text{S64})$$

Using Eq. (S64) in the second condition in Eq. (S61) gives

$$\partial_\mu \tilde{Q}_0(R_0, r + b) \Big|_{(\bar{r}, \bar{\mu})} = 0. \quad (\text{S65})$$

Equations (S63) and (S65) together determine the optimal pair of the parameters $(\bar{r}, \bar{\mu})$, or equivalently, $(\bar{r}, \bar{\alpha})$. In the following subsections, we analyze these conditions explicitly in different dimensions.

For simplicity, we consider the case of one dimension. For $d = 1$, one can take the limit of the target size going to zero. In the limit $\epsilon \rightarrow 0$ and $d = 1$, Eq. (S11) becomes

$$\tilde{Q}_0(R_0, s) = \frac{1}{s} \left[1 - \frac{2z^\mu K_\mu(2z)}{\Gamma(\mu)} \right] \quad \text{where} \quad z = \mu\sqrt{s} R_0^{\frac{1}{2\mu}}. \quad (\text{S66})$$

Using Eq. (S66) in Eq. (S63) yields,

$$2\bar{z}\bar{\mu} K_{\bar{\mu}}^2(2\bar{z}) + \bar{z}\Gamma(\bar{\mu})K_{\bar{\mu}-1}(2\bar{z}) - \Gamma(\bar{\mu})K_{\bar{\mu}}(2\bar{z}) = 0 \quad \text{where} \quad \bar{z} = \bar{\mu}\sqrt{\bar{r} + b} R_0^{\frac{1}{2\bar{\mu}}}. \quad (\text{S67})$$

Similarly, using Eq. (S66) in Eq. (S63) gives

$$\bar{\mu}^2 K_{\bar{\mu}}^{(1,0)}(2\bar{z}) + \bar{z}[\ln R_0 - 2\bar{\mu}] K_{\bar{\mu}-1}(2\bar{z}) + \bar{\mu}^2 K_{\bar{\mu}}(2\bar{z})[\ln \bar{z} - \psi^{(0)}(\bar{\mu})] = 0, \quad (\text{S68})$$

where $K_{\bar{\mu}}^{(1,0)}(2\bar{z}) = \partial_{\bar{\mu}} K_{\bar{\mu}}(2\bar{z})$ and $\psi^{(0)}(\bar{\mu})$ is the polygamma function. Solving Eqs. (S67) and (S68) together gives $\bar{\mu}$ and \bar{z} for a given R_0 , which in turn, determines the optimal parameters $\bar{r}(R_0)$ and $\bar{\mu}(R_0)$.

Given $\bar{\mu}$, Eq. (S67) determines \bar{z} uniquely. Therefore, formally we can express the optimal \bar{r} , using the last expression in Eq. (S67), as

$$\bar{r} = \left[\frac{\bar{z}(\bar{\mu})}{\bar{\mu}} \right]^2 \frac{1}{R_0^{1/\bar{\mu}}} - b. \quad (\text{S69})$$

Since the resetting rate in Eq. (S69) must be non-negative, there exists a certain R_0^* such that

$$\bar{r}(R_0) = \begin{cases} 0 & R_0 > R_0^*(\bar{\mu}) \\ \left(\frac{\bar{z}(\bar{\mu})}{\bar{\mu}} \right)^2 \frac{1}{R_0^{1/\bar{\mu}}} - b & R_0 \leq R_0^*(\bar{\mu}) \end{cases} \quad (\text{S70})$$

where

$$R_0^*(\bar{\mu}) = \left(\frac{\bar{z}(\bar{\mu})}{\bar{\mu}} \right)^{2\bar{\mu}} \frac{1}{b^{\bar{\mu}}}. \quad (\text{S71})$$

Indeed, by solving Eqs. (S67) and (S68) numerically, as shown in Fig. 3 of the main text, we find that $\bar{r} = 0$ and $\bar{\mu} = 1/2$ for large R_0 . Therefore, solving Eq. (S67) numerically with $\bar{\mu} = 1/2$, we get $\bar{z}(1/2) = 0.79681\dots$. Consequently, from Eq. (S71) we get

$$R_{02}^* \equiv R_0^*(\bar{\mu} = 1/2) = \frac{2\bar{z}(1/2)}{\sqrt{b}} = \frac{1.5936\dots}{\sqrt{b}} \quad (\text{S72})$$

From Fig. 3 (a) of the main text, there exists another critical point $R_{01}^* < R_{02}^*$ such that $\bar{\mu}$ still remains 1/2 in-between. In this range, \bar{r} is given by

$$\bar{r} = \frac{[2\bar{z}(1/2)]^2}{\sqrt{R_0}} - b \quad \text{where} \quad R_{01}^* < R_0 < R_{02}^*. \quad (\text{S73})$$

At $R_0 = R_{01}^*$, both $\bar{\alpha}$ and \bar{r} undergo a phase transition. The critical point R_{01}^* can be obtained by solving Eq. (S68) with $\bar{\mu} = 1/2$ and $\bar{z} = \bar{z}(1/2) = 0.79681\dots$. This yields

$$R_{01}^* = \exp \left\{ -\frac{\gamma E}{4\bar{z}(1/2)} + 1 - \frac{1}{4\bar{z}(1/2)} \ln[4\bar{z}(1/2)] - \frac{e^{2\bar{z}(1/2)}}{\sqrt{4\pi\bar{z}(1/2)}} K_{1/2}^{(1,0)}(2\bar{z}(1/2)) \right\} = 1.4578\dots \quad (\text{S74})$$

where $K_{1/2}^{(1,0)}(x) = \partial_{\mu} K_{\mu}(x)|_{\mu=1/2}$, which has a nice expression in terms of the exponential integral

$$K_{1/2}^{(1,0)}(x) = \sqrt{\frac{\pi}{2x}} E_1(2x)e^x, \quad \text{where} \quad E_1(x) = \int_{-\infty}^x \frac{e^t}{t} dt \quad (\text{S75})$$

is the exponential integral.

From Eqs (S72) and (S74), the condition $R_{01}^* < R_{02}^*$ demands that

$$b < b^* \quad \text{where} \quad b^* = 1.19494\dots \quad (\text{S76})$$

To summarize, for $b < b^*$, there are two critical points R_{01}^* and R_{02}^* such that

$$R_0 > R_{02}^* : \quad \bar{\alpha} = 0, \quad \bar{r} = 0 \quad (\text{S77})$$

$$R_{01}^* < R_0 < R_{02}^* : \quad \bar{\alpha} = 0, \quad \bar{r} > 0 \quad (\text{S78})$$

$$1 < R_0 < R_{01}^* : \quad \bar{\alpha} > 0, \quad \bar{r} > 0 \quad (\text{S79})$$

$$\epsilon < R_0 < 1 : \quad \bar{\alpha} \rightarrow \infty, \quad \bar{r} \rightarrow \infty \quad (\text{S80})$$

On the other hand, for $b > b^*$, a different picture emerges. There are still two critical points R_{03}^* and R_{04}^* . For $R_0 > R_{04}^*$, the optimal parameters \bar{r} and $\bar{\alpha}$ are still zero, as seen in Fig. 3 (b) of the main text. In this case, $\bar{\alpha}$ undergoes a phase transition at R_{04}^* , while \bar{r} still remains zero across R_{04}^* . Hence, the critical value R_{04}^* can be obtained by setting $\bar{\mu} = 1/2$ and $\bar{z} = \frac{1}{2}\sqrt{b} R_{04}^*$ in Eq. (S68). This yields,

$$\sqrt{\frac{2}{\pi}} b^{1/4} \sqrt{R_0} K_{1/2}^{(1,0)}(\sqrt{b} R_0) + e^{-\sqrt{b} R_0} \left[-2\sqrt{b} R_0 + \ln(2\sqrt{b} R_0) + 2\sqrt{b} R_0 \ln(R_0) + \gamma_E \right] = 0. \quad (\text{S81})$$

Equation (S81) determines R_{04}^* as a function of b for $b > b^*$. For example, for $b = 2$, numerical solution of Eq. (S81) yields, $R_{04}^* = 1.6661\dots$. The optimal value of $\bar{\alpha}$, or equivalently $\bar{\mu}$ for $R_{03}^* < R_0 < R_{04}^*$, can be obtained by solving Eq. (S68) as a function of b and R_0 , by setting $\bar{z} = \mu\sqrt{b} R_0^{\frac{1}{2\mu}}$. Fig. 3 (b) of the main text shows the optimal $\bar{\alpha}$ as a function of R_0 . When R_0 hits R_{03}^* from above, both $\bar{\alpha}$ and \bar{r} undergo another phase transition. Since \bar{r} undergoes a zero to non-zero transition at R_{03}^* , from Eq. (S71), R_{03}^* should self-consistently satisfy the relation

$$R_{03}^* = \left(\frac{\bar{z}(\mu^*)}{\mu^*} \right)^{2\mu^*} \frac{1}{b^{\mu^*}} \quad \text{where} \quad \mu^* = \bar{\mu}(R_{03}^*). \quad (\text{S82})$$

This can indeed be checked at the critical point R_{03}^* for $b = 2$ in Fig. 3 (b) of the main text.

To summarize, for $b > b^*$, we have

$$R_0 > R_{04}^* : \quad \bar{\alpha} = 0, \quad \bar{r} = 0 \quad (\text{S83})$$

$$R_{03}^* < R_0 < R_{04}^* : \quad \bar{\alpha} > 0, \quad \bar{r} = 0 \quad (\text{S84})$$

$$1 < R_0 < R_{03}^* : \quad \bar{\alpha} > 0, \quad \bar{r} > 0 \quad (\text{S85})$$

$$\epsilon < R_0 < 1 : \quad \bar{\alpha} \rightarrow \infty, \quad \bar{r} \rightarrow \infty \quad (\text{S86})$$

A similar analysis can be performed in higher dimensions, but there is an additional parameter ϵ .

-
- [1] A. Zodage, R. J. Allen, M. R. Evans, and S. N. Majumdar, *J. Stat. Mech.*, 033211 (2023).
 - [2] G. Del Vecchio Del Vecchio and S. N. Majumdar, *J. Stat. Mech.*, 023207 (2025).
 - [3] A. L. Stella, A. Chechkin, and G. Teza, *Phys. Rev. Lett.* **130**, 207104 (2023).
 - [4] A. L. Stella, A. Chechkin, and G. Teza, *Phys. Rev. E* **107**, 054118 (2023).
 - [5] L. Menon and C. Anteneodo, *Phys. Rev. E* **110**, 054111 (2024).
 - [6] M. Abramowitz and I. Stegun, *Handbook of Mathematical Functions: With Formulas, Graphs, and Mathematical Tables*, Applied mathematics series (Dover Publications, 1965).
 - [7] S. Redner, *A Guide to First-Passage Processes* (Cambridge University Press, 2001).
 - [8] A. J. Bray, S. N. Majumdar, and G. Schehr, *Adv. Phys.* **62**, 225 (2013).